Alexander Mertsch, Sebastian Letschert, Elisabeth Memmel, Markus Sauer and Jürgen Seibel*

Synthesis and application of water-soluble, photoswitchable cyanine dyes for bioorthogonal labeling of cell-surface carbohydrates

DOI 10.1515/znc-2016-0123
Received June 14, 2016; revised July 28, 2016; accepted July 28, 2016

Abstract: The synthesis of cyanine dyes addressing absorption wavelengths at 550 and 648 nm is reported. Alkyne functionalized dyes were used for bioorthogonal click reactions by labeling of metabolically incorporated sugar-azides on the surface of living neuroblastoma cells, which were applied to *direct* stochastic optical reconstruction microscopy (*d*STORM) for the visualization of cell-surface glycans in the nm-range.

Keywords: bioorthogonal chemistry; click chemistry; cyanine dyes; membrane glycans; microscopy; super-resolution imaging.

Dedication: This work is dedicated to the memory of Professor Peter Böger.

1 Introduction

The surface of eukaryotic cells is highly decorated with glycan structures of various types forming the glycocalyx. Cell-surface glycans have been shown to participate in cell-cell recognition processes and tumor development. They also reflect the developmental stage and the transformation state of a cell [1–3]. It is of particular interest where on the cell-surface interacting human proteins are located and what their binding partners are. Bertozzi and coworkers have shown that functionalized carbohydrates can be incorporated into cells in vitro by active transporters and diffusion procedures [4, 5]. She introduced the term bioorthogonal chemistry, which refers to any chemical reaction that can occur inside of living systems without interfering with native biochemical processes [6]. We like to use special synthesized carbohydrate labels, which, in combination with new super-resolution imaging, allow the identification of cell-surface glycans well below the diffraction limit approaching virtually molecular resolution.

Fluorescent reporter technologies are emergent tools to follow cellular processes in vivo [7]. However, optical imaging methods are often limited by poor sensitivity and high background noise due to limited binding specificity and insufficient optical resolution [8]. These limitations can be overcome using small covalently attached fluorescent probes with short linkers in combination with new super-resolution fluorescence microscopy methods [9, 10].

Cyanine dyes belong to the family of long-known polymethine dyes [11, 12]. In general, they consist of two heterocyclic rings containing nitrogen centers, which are linked by a conjugated chain of methine groups [12, 13]. They are well known for their excellent spectral properties including broad wavelength tunabilities, sharp fluorescence bands, stability and high sensitivity [14, 15].

Introduction of vinylsulfone groups and functionalized side chains can be used to generate all required properties such as good water solubility and specific functionalities. Vinylsulfone groups ensure excellent water solubility and prevent self-aggregation in aqueous environment as described for cyanine dyes with intrinsic hydrophobicity [15–17]. To introduce specific functionalities that can selectively react with the target molecule we wish to observe, side chains can be introduced directly to the nitrogen centers. The alkylated indoles can be used like a modular system to be connected by a variable polymethine chain. Using this system, the absorption wavelength can be varied from ~450 nm (m = 0) to ~750 nm (m = 3).

Even though many different cyanine dyes have been synthesized [15–18] and some photoswitchable cyanine dyes are commercially available, as far as we know, there is no literature about the synthesis of alkyne

***Corresponding author: Jürgen Seibel,** Institute of Organic Chemistry, Julius-Maximilians-University Würzburg, Am Hubland, 97074 Würzburg, Germany, E-mail: seibel@chemie.uni-wuerzburg.de
Alexander Mertsch and Elisabeth Memmel: Institute of Organic Chemistry, Julius-Maximilians-University Würzburg, Am Hubland, 97074 Würzburg, Germany
Sebastian Letschert and Markus Sauer: Department of Biotechnology and Biophysics, Julius-Maximilians-University Würzburg, 97074 Würzburg, Germany

functionalized side chains in water-soluble cyanine dyes. Herein we report the feasible quantitative scale synthesis of photoswitchable alkyne functionalized water-soluble cyanine dyes with absorption wavelengths from ~550 (m = 1) to ~650 nm (m = 2) which have been used successfully for the bioorthogonal Huisgen-Meldal-Sharpless click reaction on the surface of living cells.

2 Experimental

2.1 General

All chemicals were purchased from Sigma-Aldrich (St. Louis, MO, USA), Thermo Fisher Scientific (Waltham, MA, USA) and Merck (Darmstadt, Germany). All solvents were distilled prior to use and dried if necessary.

Thin layer chromatography (TLC) was performed on aluminum sheets with TLC silica gel 60F_{254} and on aluminum plates-RP-18 F_{254} from Merck.

Normal-phase column chromatography was performed on silica gel 60 M, 40–63 µm (230–400 mesh) from Macherey-Nagel (Düren, Germany). Reversed-phase column chromatography was performed on C18-RP silica gel, 17% C, 0.8 mmol/g, 40–63 µm from Acros Organics (Geel, Belgium). Nuclear magnetic resonance (NMR) spectra were obtained with Bruker Avance 400 (400 MHz) and Bruker DMX 600 (600 MHz) instruments (Bremen, Germany). The chemical shifts are reported in parts per million with calibration to the used solvent [19]. ^{13}C-Spectra measured in D_2O were calibrated to added acetone. Coupling constants are reported in Hertz.

ESI-TOF mass spectrometry was performed with Bruker Daltonics micrOTOF.

Absorption spectra were determined using a JASCO V-670 (Easton, MD, USA). Emission spectra were determined by PTI, LPS-220B from Photon Technology International (Edison, NJ, USA) as light source, Photomultiplier type R928P and Xenon short arc lamp UXL-75XE from Ushio (Oude Meer, Netherlands).

2.2 Synthesis

The detailed synthesis of compounds **1–6** is shown in the supporting information. Synthesis of compounds **2**, **3** and **5**, **6** has been reported earlier [18].

Potassium-3,3-dimethyl-2-((1*E*,3*E*)-4-(*N*-phenylacetamido)buta-1,3-dien-1-yl)-1-(4-sulfonatobutyl)-3*H*-indolium-5-sulfonate (7): Potassium-1-(4-sulfonatobutyl)-2,3,3-trimethyl-3*H*-indolium-5-sulfonate (500 mg, 1.21 mmol; **5**) and *N*-[(2*E*)-3-(phenylamino)-2-propen-1-ylidene]- benzenamine hydrochloride (360 mg, 1.40 mmol; **4**) were heated to 120°C in a mixture of acetic acid (5 mL) and acetic anhydride (5 mL) for 60 min. After reaching room temperature, the solvent was removed on a rotary evaporator. The obtained solid was washed with ethyl acetate and dried under high vacuum in the dark. Owing to its instability, the resulting green-brown product was used immediately in the next reaction without further purification (390 mg ≙ ca. 50%) R_f = 0.52 (RP-C18, H_2O/MeOH = 3:1); ^{1}H-NMR (D_2O, 400 MHz): δ = 8.50 (d, *J* = 13.3 Hz, 1H, *H*-4″), 8.29 (dd, *J* = 14.9 Hz, 11.4 Hz, 1H, *H*-2″), 8.03 (d, *J* = 1.7 Hz, 1H, *H*-4), 7.96 (dd, *J* = 8.5 Hz, 1.7 Hz, 1H, *H*-6), 7.69 (d, *J* = 8.5 Hz, 1H, *H*-7), 7.65 (m, 2H, *H*-2^{IV}), 7.35 (dd, *J* = 8.1 Hz, *J* = 1.5 Hz, 2H, *H*-1^{IV}), 7.29 (dd, *J* = 8.1 Hz, *J* = 1.5 Hz, 1H, *H*-3^{IV}), 6.58 (d, *J* = 14.9 Hz, 1H, *H*-1″), 5.66 (dd, *J* = 11.4 Hz, 13.3 Hz, 1H, *H*-3″), 4.27 (t, *J* = 7.6 Hz, 2H, *H*-1′), 2.87 (t, *J* = 7.5 Hz, 2H, *H*-4′), 2.27 (s, 3H, *H*-2^{V}), 1.96–1.89 (m, 2H, *H*-3′), 1.80–1.76 (m, 2H, *H*-2′), 1.73 (s, 6H, *H*-1‴) ppm.

2-[(1*E*,3*E*,5*E*)-5-(1-(5-carboxypentyl)-3,3-dimethyl-5-sulfonato-2*H*-indole-2-yliden)penta-1,3-dien-1-yl]-3,3-dimethyl-1-(4-sulfonatobutyl)-3*H*-indolium-5-sulfonate (8a): The hemicyanine intermediate (2.90 g, 4.96 mmol; **7**) was dissolved in a mixture of acetic anhydride (30 mL) and pyridine (15 mL) and potassium-1-(5-carboxypentyl)-2,3,3-trimethyl-3*H*-indolium-5-sulfonate (2.00 g, 5.10 mmol; **6**) was added. The reaction mixture was heated to 120°C for 100 min under nitrogen atmosphere in the dark. After cooling to room temperature, ethyl acetate was added to precipitate a blue solid. It was filtered, washed with ethyl acetate and isopropyl alcohol and dried under high vacuum. The raw product was purified by reversed-phase column chromatography to obtain a dark blue solid (46.0 mg, 60.1 µmol, 9% from 449 mg raw product). R_f = 0.58 (RP-C18, H_2O/MeOH = 4:1); ^{1}H-NMR (D_2O, 600 MHz): = 7.92 (m, 2H, *H*-2″/4″), 7.79 (s, 2H, *H*-4/4^{IV}), 7.76 (d, *J* = 8.3 Hz, 2H, *H*-6/6^{IV}), 7.31 (d, *J* = 8.3 Hz, 2H, *H*-7/7^{IV}), 6.48 (t, *J* = 12.3 Hz, 1H, *H*-3″), 6.16 (d, *J* = 13.3 Hz, 1H, *H*-1″/5″), 4.05 (m, 4H, *H*-1′/1^{V}), 2.97 (t, *J* = 7.2 Hz, 2H, *H*-4′), 2.24 (t, *J* = 6.3 Hz, 2H, *H*-5^{V}), 1.89 (m, 4H, *H*-2′/3′), 1.76 (m, 2H, *H*-2^{V}), 1.61 (m, 2H, *H*-4^{V}), 1.56 (s, 12H, *H*-1‴/1^{VI}), 1.40 (m, 2H, *H*-3^{V}) ppm. ^{13}C-NMR (D_2O, 150 MHz): δ = 182.39 (*C*-6^{V}), 174.70 (*C*-2), 174.23 (*C*-2^{IV}), 155.10 (*C*-2″), 154.87 (*C*-4″), 144.82 (*C*-7a/7a^{IV}), 142.47 (*C*-3a), 142.34 (*C*-3a^{IV}), 139.91 (*C*-5), 139.69 (*C*-5^{IV}), 120.39 (*C*-4/4^{IV}), 126.39 (*C*-3″), 127.13 (*C*-6/6^{IV}), 111.80 (*C*-7), 111.54 (*C*-7a^{IV}), 104.92 (*C*-1″), 104.58 (*C*-5″), 51.11 (*C*-4′), 49.76 (*C*-3), 49.63 (*C*-3^{IV}), 44.76 (*C*-1′), 44.31 (*C*-1^{V}), 36.81 (*C*-5^{V}), 27.47 (*C*-1‴), 27.38 (*C*-1^{VI}), 27.28 (*C*-2^{V}), 26.53 (*C*-3^{V}), 26.23 (*C*-3′), 25.83 (*C*-4^{V}),

22.34 (*C*-2′) ppm. ESI-MS m/z 381.09837 ($C_{35}H_{42}N_2O_{11}S_3^{2-}$ requires 381.09808).

2-((1*E*,3*E*,5*E*)-5-(1-(6-oxo-6-(prop-2-yne-1-amino) hexyl)-3,3-dimethyl-5-sulfonato-2*H*-indole-2-yliden) penta-1,3-dien-1-yl)-3,3-dimethyl-1-(4-sulfonatobutyl)-3*H*-indolium-5-sulfonate (8b): The cyanine dye (56.0 g, 73.2 µmol, **8a**) was dissolved in *N*,*N*-dimethylformamide (5 mL) and *N*,*N*-diisopropylethylamine (15 mg, 148 µmol), HBTU (35.0 mg, 92.3 µmol) and propargylamine (7.00 mg, 127 µmol) were added. The reaction mixture was stirred for 22 h at room temperature. Diethyl ether was added to precipitate a blue solid which was centrifuged. For purification, reversed-phase column chromatography was used. Separation from **8a** could not be achieved. NMR-spectra reported that a mixture of **8a** and **8b** was obtained [25.0 mg (1:1 8a/8b ≙ 12.5 mg, 15.6 µmol, 21%)]. R_f = 0.38 (RP-C18, H_2O/MeOH = 4:1); ^{1}H-NMR (D_2O, 600 MHz): = 7.94 (m, 2H, *H*-2″/4″), 7.80 (s, 2H, *H*-4/4^{IV}), 7.77 (d, *J* = 8.1 Hz, 2H, *H*-6/6^{IV}), 7.29–2.32 (m, 2H, *H*-7/7^{IV}), 6.49 (t, *J* = 12.4 Hz, 1H, *H*-3″), 6.16 (d, *J* = 14.1 Hz, 1H, *H*-1″/5″), 4.00–4.07 (m, 4H, *H*-1′/1^{V}), 3.83 (s, 2H, *H*-8^{V}), 2.96–2.98 (m, 2H, *H*-4′), 2.52 (m, 1H, *H*-10^{V}), 2.20 (t, *J* = 7.1 Hz, 2H, *H*-5^{V}), 1.85–1.94 (m, 4H, *H*-2′/3′), 1.74–1.81 (m, 2H, *H*-2^{V}), 1.61–1.62 (m, 2H, *H*-4^{V}), 1.59 (2s, 12H, *H*-1‴/1^{VI}), 1.29–1.33 (m, 2H, *H*-3^{V}) ppm. ^{13}C-NMR (D_2O, 150 MHz): δ = 176.86 (*C*-6^{V}), 174.60 (*C*-2^{IV}), 174.38 (*C*-2), 154.91 (*C*-2″/4″), 144.73 (*C*-7a/7a^{IV}), 142.37 (*C*-3^{IV}), 142.34 (*C*-3), 139.79 (*C*-5^{IV}), 139.70 (*C*-5), 120.34 (*C*-4/4^{IV}), 126.36 (*C*-3″), 127.08 (*C*-6/6^{IV}), 111.79 (C-7^{IV}), 111.53 (*C*-7), 104.84 (*C*-5″), 104.66 (*C*-1″), 80.29 (*C*-9^{V}), 72,41 (*C*-10^{V}), 51.02 (*C*-4′), 49.68 (*C*-3a^{IV}), 49.63 (*C*-3a), 44.53 (*C*-1^{V}), 44.29 (*C*-1′), 35.34 (*C*-5^{V}), 29.26 (*C*-8^{V}), 27.40 (*C*-1^{VI}), 27.35 (C-1‴), 27.08 (*C*-2^{V}), 26.14 (*C*-3^{V}), 26.06 (*C*-3′), 25.44 (*C*-4^{V}), 22.29 (*C*-2′) ppm. ESI-MS m/z 399.61420 ($C_{38}H_{45}N_3O_{10}S_3^{2-}$ requires 399.61390).

Potassium-3,3-dimethyl-2-((*E*)-2-(*N*-phenylamino) vinyl)-1-(4-sulfonatobutyl)-3*H*-indolium-5-sulfonate (9): Potassium-1-(4-sulfonatobutyl)-2,3,3-trimethyl-3*H*-indolium-5-sulfonate (600 mg, 1.60 mmol; **5**) and *N*,*N*′-diphenylformamidine (370 mg, 1.88 mmol) were suspended in ethanol (10 mL) and mixed with triethoxymethane (300 mg, 2.02 mmol). This mixture was heated to reflux for 6 h and afterward cooled on ice. For complete crystallization, diethyl ether was added. The orange solid was filtered, washed with diethyl ether and dried under high vacuum. For NMR-characterisation, a small amount was purified by reversed-phase column chromatography. The raw product was used without further purification (550 mg). R_f = 0.38 (RP-C18, H_2O/MeOH = 4:1); ^{1}H-NMR (D_2O, 400 MHz): δ = 8.65 (d, *J* = 12.5 Hz, 1H, *H*-2″), 7.96 (d, *J* = 1.7 Hz, 1H, *H*-4), 7.93 (dd, *J* = 8.4 Hz, *J* = 1.7 Hz, 1H, *H*-6), 7.54 (m, 2H, *H*-5″), 7.49 (d, *J* = 8.4 Hz, 1H, *H*-7), 7.41 (m, 2H, *H*-6″), 7.37 (m, 1H, *H*-7″), 6.21 (d, *J* = 12.5 Hz, 1H, *H*-1″), 4.21 (t, *J* = 7.2 Hz, 2H, *H*-1′), 3.02 (t, *J* = 7.4 Hz, 2H, *H*-4′), 2.04 (m, 2H, *H*-3′), 1.94 (m, 2H, *H*-2′), 1.77 (s, 6H, *H*-1‴) ppm. ^{13}C-NMR (D_2O, 100 MHz): δ = 179.52 (*C*-2), 153.09 (*C*-2″), 143.80 (*C*-7a), 141.51 (*C*-3a), 139.80 (*C*-5), 138.03 (*C*-4″), 129.99 (*C*-6″), 126.88 (*C*-7″), 126.57 (*C*-6), 119.83 (*C*-4), 118.22 (*C*-5″), 111.65 (*C*-7), 91.37 (*C*-1″), 50.29 (*C*-4′), 49.67 (*C*-3), 43.97 (*C*-1′), 27.53 (*C*-1‴), 25.21 (*C*-3′), 21.64 (*C*-2′) ppm.

2-((1*E*,3*E*)-3-(1-(5-carboxypentyl)-3,3-dimethyl-5-sulfonato-2H-indole-2-yliden)prop-1-en-1-yl)-3,3-dimethyl-1-(4-sulfonatobutyl)-3*H*-indolium-5-sulfonate (10a): The hemicyanine intermediate (1.39 g, 2.49 mmol; **9**) was dissolved in a mixture of acetic anhydride (8 mL) and pyridine (8 mL) and potassium-1-(5-carboxypentyl)-2,3,3-trimethyl-3*H*-indolium-5-sulfonate (1.19 g, 3.11 mmol; **6**) was added. The reaction mixture was heated to 110°C for 120 min under nitrogen atmosphere in the dark. After cooling to room temperature diethyl ether was added to precipitate a pink solid. It was filtered, washed with isopropyl alcohol and dried under high vacuum. The raw product was repeatedly purified by reversed-phase column chromatography to obtain a pink solid (23.0 mg, 31.1 µmol, 17% from 137 mg raw product). R_f = 0.62 (RP-C18, H_2O/MeOH = 4:1); ^{1}H-NMR (D_2O, 400 MHz): δ = 8.53 (t, *J* = 13.5 Hz, 1H, *H*-2″), 7.93 (m, 2H, *H*-4/4^{IV}), 7.88 (dm, *J* = 8.4 Hz, 2H, *H*-6/6^{IV}), 7.40, 7.38 (d,d *J* = 8.4 Hz, 2H, *H*-7/7^{IV}), 6.42 (d, *J* = 13.5 Hz, 2H, *H*-1″/3″), 4.09–4.16 (m, 4H, *H*-1^{V}), 3.00 (t, *J* = 7.3 Hz, 2H, *H*-4′), 2.36 (t, *J* = 7.3 Hz, 2H, *H*-5^{V}), 1.94–2.01 (m, 2H, *H*-2′), 1.89–1.94 (m, 2H, *H*-3′), 1.81–1.87 (m, 2H, *H*-2^{V}), 1.74, 1.75 (s, s, 12H, *H*-1‴/1^{VI}), 1.62–1.67 (m, 2H, *H*-4^{V}), 1.40–1.46 (m, 2H, *H*-3^{V}) ppm. ^{13}C-NMR (D_2O, 100 MHz): δ = 179.21 (*C*-6^{V}), 176.01 (*C*-2^{IV}), 175.74 (*C*-2), 151.97 (C-2″) 144.09 (*C*-7a^{IV}), 144.02 (*C*-7a), 141.56 (*C*-5^{IV}), 141.50 (*C*-5), 139.63 (*C*-3a^{IV}), 139.50 (*C*-3a), 126.65 (*C*-6/6^{IV}), 119.81 (*C*-4/4^{IV}), 111.54 (*C*-7^{IV}), 111.37 (*C*-7), 103.75 (*C*-3″), 103.45 (*C*-1″), 50.42 (*C*-4′), 49.32 (*C*-3^{IV}), 49.25 (*C*-3), 44.11 (*C*-1^{V}), 43.81 (*C*-1′), 34.09 (*C*-5^{V}), 27.11 (*C*-1^{VI}), 27.05 (*C*-1″), 26.41 (*C*-2^{V}), 25.57 (*C*-2′), 25.46 (C-3^{V}), 24.22 (*C*-4^{V}), 21.64 (*C*-3′) ppm. ESI-MS m/z 368.09042 ($C_{33}H_{40}N_2O_{11}S_3^{2-}$ requires 368.09026).

During purification of **10a** the symmetrical dye with two sulfonatobutyl chains at the nitrogen center of the indole (**10b**) was isolated and characterized. R_f = 0.82 (RP-C18, H_2O/MeOH = 4:1); ^{1}H-NMR (D_2O, 400 MHz): δ = 8.63 (t, *J* = 13.4 Hz, 1H, *H*-2″), 7.96 (d, *J* = 1.8 Hz, 2H, *H*-4/4^{IV}), 7.91 (dd, *J* = 8.4 Hz, *J* = 1.8 Hz, 2H, *H*-6/6^{IV}), 7.47 (d *J* = 8.4 Hz, 2H, *H*-7/7^{IV}), 6.48 (d, *J* = 13.4 Hz, 2H, *H*-1″/3″), 4.23 (m, 4H, *H*-1′/1^{V}), 3.03 (m, 4H, *H*-4′/4^{V}), 1.99–2.11 (m, 4H, *H*-2′/2^{V}), 1.90–1.97 (m, 4H, *H*-3′/3^{V}), 1.83 (s, 12H, *H*-1‴/1^{VI}) ppm. ^{13}C-NMR (D_2O, 100 MHz): δ = 176.07 (*C*-2/2^{IV}), 152.32

(*C*-2″), 144.27 (*C*-7a/7a^{IV}), 141.72 (*C*-3/3a^{IV}), 139.32 (*C*-5/5^{IV}), 126.57 (*C*-6/6^{IV}), 119.80 (*C*-4/4^{IV}), 111.42 (*C*-7/7^{IV}), 103.65 (*C*-1″/3″), 50.47 (*C*-4′/4^{V}), 49.36 (*C*-2/2^{IV}), 43.88 (*C*-1′/1^{V}), 27.10 (*C*-1‴/1^{VI}), 25.59 (*C*-2′/2^{V}), 21.67 (*C*-3′/3^{V}) ppm. ESI-MS m/z 398.04128 ($C_{31}H_{37}KN_2O_{12}S_4^{2-}$ requires 398.04277).

2.3 Metabolic glycoengineering and click-reaction

Neuroblastoma cells (SK-N-MC) were cultivated in RPMI-1640 medium supplemented with sodium pyruvate, 10% FCS, 4 mM glutamine, 100 U/mL penicillin and 0.1 mg/mL streptomycin at 37°C under 5% CO_2. For metabolic glycoengineering, cells were incubated in LabTek II chamber slides with 25 μM acetylated *N*-azidoacetyl-glucosamine (Ac_4GlcNAz) for 2 days. For fluorescent staining of metabolized cell-surface sugar azides, cells were washed once with PBS and then incubated with 25 μM dye **8b**, 50 μM $CuSO_4$, 250 μM tris(3-hydroxypropyltriazolylmethyl) amine (THPTA) and 2.5 mM sodium ascorbate in PBS for 5 min at RT. Afterward, the staining solution was removed, cells were washed three times with PBS and then fixed for 1 h with 4% formaldehyde and 0.2% glutaraldehyde at RT. Finally, cells were washed three times with PBS.

2.4 Super-resolution imaging

*d*STORM measurements were performed as described in the literature [20, 21]. Briefly, we used an Olympus IX-71 inverted microscope equipped with an oil-immersion objective (PlanApo 60×, NA 1.45, Olympus, Tokyo, Japan). The cyanine dye **8b** was excited with a 641 nm diode laser (Cube 640–100C; Coherent, Santa Clara, CA, USA). A Clean-up filter was inserted into the excitation path (Laser Clean-up filter 640/10; Chroma, Bellows Falls, VT, USA), which was then focused onto the backfocal plane of the objective. A dichroic mirror (HC 410/504/582/669; Semrock, Lake Forest, IL, USA) was used to separate the fluorescence and excitation light. The fluorescence emission was collected by the same objective and filtered by a bandpass filter (LP647 + FF01-697/75, Semrock), before being projected on an electron-multiplying CCD camera (iXon DU-897; Andor, Belfast, UK). The final pixel size of 133 nm was generated by placing additional lenses in the detection path. Excitation intensities were in the range of 1–5 kW/cm^2. Typically, 15,000 frames were measured with a frame rate of 50 Hz using total internal reflection fluorescence (TIRF) microscopy. For reversible photoswitching of the dye **8b**, a PBS-based imaging buffer (pH 7.4) was used which contained 80 mM β-mercaptoethylamine (MEA; Sigma-Aldrich) and an oxygen scavenger system containing 2% (w/v) glucose, 4 U/mL glucose oxidase and 80 U/mL catalase. From the recorded image stack, a reconstructed *d*STORM image was generated using the open source software rapi*d*STORM 3.3 [22]. Only fluorescent spots containing more than 500 photons per frame were analyzed.

3 Results and discussion

3.1 Synthesis of polymethine dyes

A major difficulty in the development of cyanine dyes is the realization of water solubility and stability at the same time [23]. Increasing length of the polymethine chain correlates with instability [23]. It is known that incorporation of a cyclohexenyl or cyclopentenyl ring in the polymethine chain increases the stability of heptamethine cyanine dyes [23–25]. Unfortunately, these groups lead to aggregation in aqueous solution which is indicated by a loss of sharp absorption bands equivalent to loss of fluorescence [26]. Beside the effect of excellent water solubility, sulfonic acid groups increase fluorescent quantum yield and decrease the dependence of the fluorescence on the chemical environment [27]. Therefore, pentamethine and trimethine cyanine dyes with no branched polymethine chain, containing sulfonic acid groups at the indole ring, were synthesized. The synthesis was commenced with hydrazinobenzenesulfonic acid to start the formation of the indole. An overview of the cyanine dyes developed in this work is shown in Table 1.

After the synthesis of 4-hydrazinobenzenesulfonic acid (**1**), Fisher indole synthesis with 3-methyl-2-butanone

Table 1: Chemical structures of cyanine dyes synthesized in this work.

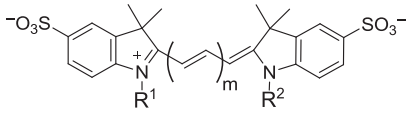

Dye compound	m	R^1	R^2
8a	2	$-(CH_2)_4SO_3^-$	$-(CH_2)_5COOH$
8b	2	$-(CH_2)_4SO_3^-$	$-(CH_2)_5CONH(CH_2)C(CH)$
10a	1	$-(CH_2)_4SO_3^-$	$-(CH_2)_5COOH$
10b	1	$-(CH_2)_4SO_3^-$	$-(CH_2)_4SO_3^-$

was performed to obtain 2,3,3-trimethyl-3*H*-indole-5-sulfonic acid (**2**). After cation exchange to potassium, sulfonate alkylation was performed by refluxing in 1,2-dichlorbenzene to introduce a carboxylic acid group (**6**) or an additional sulfonate group (**5**) for excellent water solubility. Therefore butane sultone or 6-bromohexanoic acid were used.

The alkylated indoles can be used like a modular system. Reflux with *N*-[(2*E*)-3-(phenylamino)-2-propen-1-ylidene]-benzenamine hydrochloride (**4**) in a mixture of acetic acid and acetic anhydride, or alternatively *N*,*N*′-diphenylformamidine in triethoxymethane, give the according hemicyanines (**7, 9**). Subsequent condensation in a mixture of acetic anhydride and pyridine at 110°C–120°C with a second indole gives cyanine dyes with three or five methine groups. Cyanines with carboxylic acid can be functionalized by amidation with propargylamine to give the terminal alkyne (**8b**, Scheme 1).

Isolation of the cyanine dyes proved to be very difficult, as side products and cleavage products had nearly the same polarity. Under too harsh conditions, the side chains at the nitrogen centers of the indole ring can be split off as we could observe in ESI-MS spectra.

3.2 Metabolic glycoengineering and cell microscopy

To demonstrate that the synthesized dyes can be used for labeling of cell-surfaces, metabolic glycoengineering was applied to neuroblastoma cells (SK-N-MC) with acetylated *N*-azidoacetyl-glucosamine ($Ac_4GlcNAz$) (Figure 1A). In this approach, sugars containing a bioorthogonal side chain (like azide or alkyne) are added to the cell culture medium [28, 29]. The cells take up the carbohydrates and metabolize them like their natural equivalents, while the tag is not altered. This approach has been shown with $Ac_4GalNAz$, $Ac_4ManNAz$ and $Ac_4GlcNAz$ before, and very recently high resolution microscopy was applied [30–32]. $Ac_4GlcNAz$ enters the cell metabolism after cleavage of the acetyl groups by esterases and is metabolized in various pathways. On the one hand, it can be incorporated into

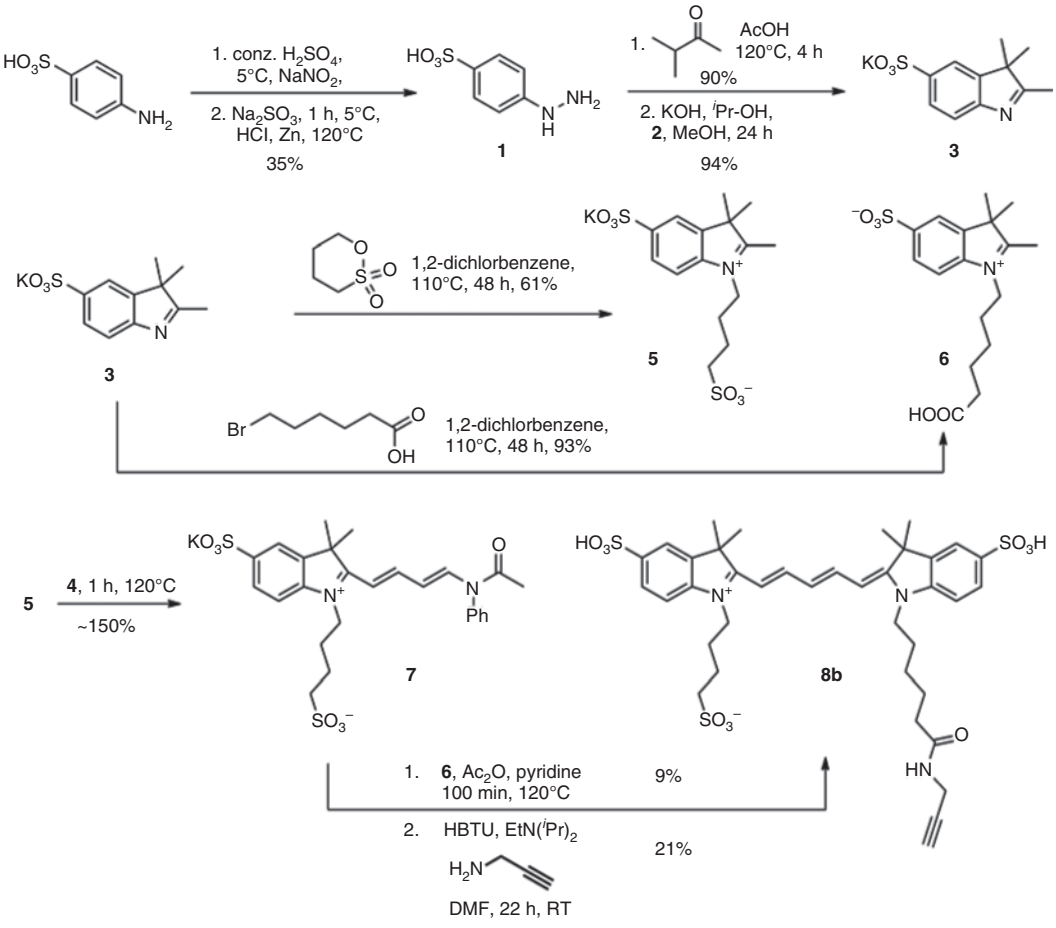

Scheme 1: Synthesis of photoswitchable alkyne cyanine **8b**.

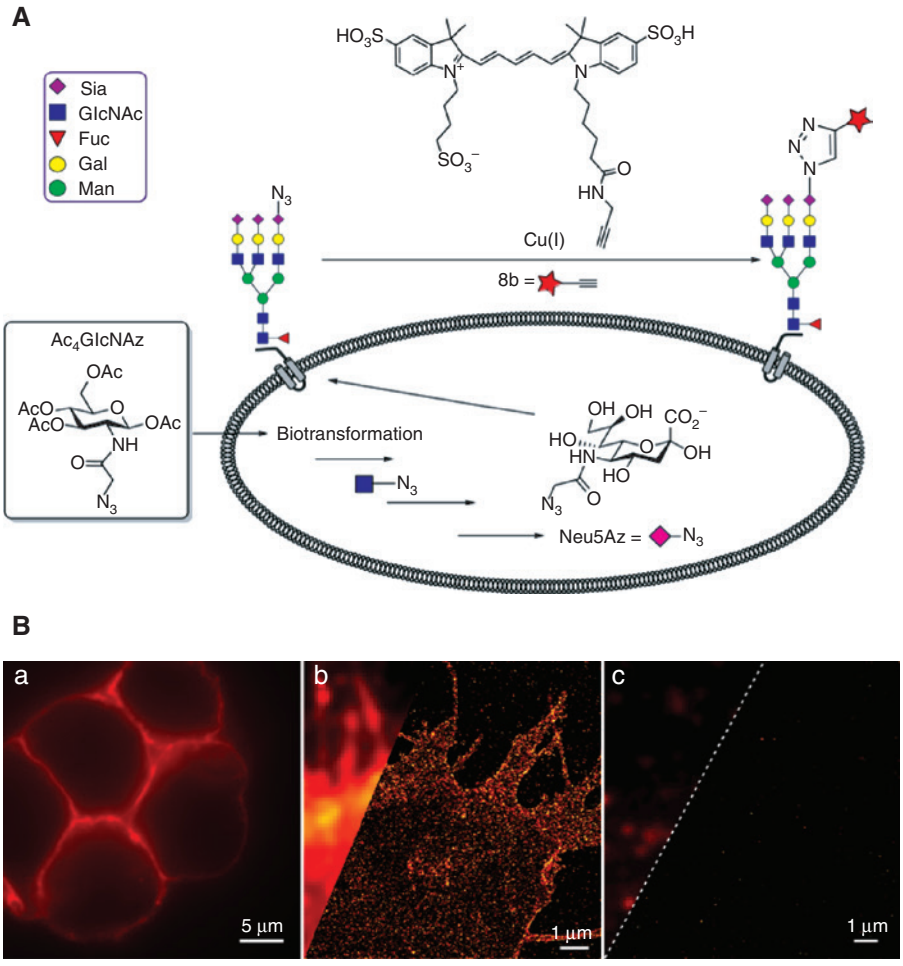

Figure 1: Detection of cell-surface staining with fluorescence microscopy and superresolution imaging.
(A) Metabolic glycoengineering of SK-N-MC with Ac_4GlcNAz and bioorthogonal labeling with **8b**. Schematic illustration of the principles of metabolic glycoengineering: The acetylated carbohydrate analog Ac_4GlcNAz enters the cell, is biotransformed to the sialic acid Neu5Az in the Golgi and finally presented in the cell-surface glycans [19, 21]. Labeling is performed by Click-reaction with the synthesized cyanine dye **8b**. (B) Membrane glycans of neuroblastoma cells stained via metabolic incorporation of Ac_4GlcNAz and copper-catalyzed azide-alkyne cycloaddition (CuAAC). (a) Conventional fluorescence image with the focal plane in the center of the cell (far above the glass surface/basal membrane). It is seen that there is no fluorescence signal in the cytoplasm. (b) The standard fluorescence image (left part) shows bright staining of the cell-surface, whereas *d*STORM enables high-resolution imaging of membrane-associated glycans (right part) proving **8b** to be photoswitchable. (c) The negative control without Ac_4GlcNAz shows only few spots coming from single fluorophores sticking unspecifically to the glass surface. The images in (b) and (c) were recorded in the TIRF mode.

cell-surface N- and O-linked glycans as Neu5Az or directly as GlcNAz [4, 29, 31, 33]. On the other hand, many cytosolic O-linked glycans can incorporate GlcNAz residues [34, 35]. Although Ac_4ManNAz is known for higher cell-surface incorporation rates, we used Ac_4GlcNAz to demonstrate the ability of our dye to discriminate between intracellular and cell-surface glycan products expressed from Ac_4GlcNAz bearing the azide side chain. The dye proved to be applicable for selective cell-surface staining.

The tagged carbohydrates are partly incorporated into cell-surface glycan structures and present the bioorthogonal side chain that can be reacted with the appropriate counterpart (alkyne) in a [3+2]-cycloaddition by copper catalyzed azide-alkyne cycloaddition (CuAAc) [4, 31, 33, 36–38].

The azide presented on the cell-surface was stained in a selective click reaction with **8b**. As we used living cells in the staining experiments, we investigated copper(I) up to 50 µM as non toxic. Cell-surface staining by copper-catalyzed azide-alkyne cycloaddition (CuAAc) was detected with fluorescence microscopy and superresolution imaging by *d*STORM. *d*STORM requires fluorescent dyes which can be reversibly switched between a fluorescent "on" state and a dark "off" state upon irradiation in the presence of millimolar concentrations of thiols [20, 21]. Because only a sparse subset of fluorophores is

residing in the "on" state at any time of the experiment, temporally and spatially separated point-spread functions (PSFs) can be fit (localized) individually using a 2D-Gaussian approximation. Finally, a super-resolved image is reconstructed from all localizations determined during the experiment [20, 21]. While the negative control shows only some unspecific fluorescence signals, labeled cells show a quite homogeneous distribution of glycans on the cell membrane as expected and previously shown [30] (Figure 1B). Live-cell imaging with this dye is possible for a range of fluorescence microscopy techniques, as for example conventional fluorescence imaging, confocal laser-scanning microscopy and also *d*STORM. In the special case of *d*STORM one caution is that under live-cell conditions the reducing buffer environment can affect cell integrity. By using the thiol glutathione, which is present in living cells at concentrations of 1–11 mM, harsh buffer conditions as used for fixed cells can be circumvented [39, 40].

3.3 Spectral properties

All absorption and emission maxima were determined in water. The maximum intensity of absorption and emission were set manually to 1 because there was no interest to compare them. Absorption maxima for compounds with five methine groups were at 648–650 nm with a shoulder at 600–630 nm. Expectedly, the decrease of the polymethin chain by two units leads to a shift of about 100 nm. Absorption maxima for cyanine dyes with three methine groups therefore were in a range of 550 nm with a shoulder at 510–525 nm. The variation of side chains between **8a** and **8b** as well as **10a** and **10b** causes only a marginal difference of the absorption maximum. For emission wavelength measurement, **8a** and **8b** were illuminated with red laser light of 610 nm. Cy3-compounds **10a** and **10b** were illuminated with green laser light of 520 nm. Both are prominent usable wavelengths for excitation with a helium-neon laser. Because of the small Stokes shift of only 16–23 nm, which is a distinctive range for cyanine dyes, the illumination wavelength was chosen to be not the exact absorption maximum. Accurate absorption and emission maxima are shown in Table 2.

Table 2: Absorption and emission maxima of cyanine dyes **8a**/**b** and **10a**/**b**.

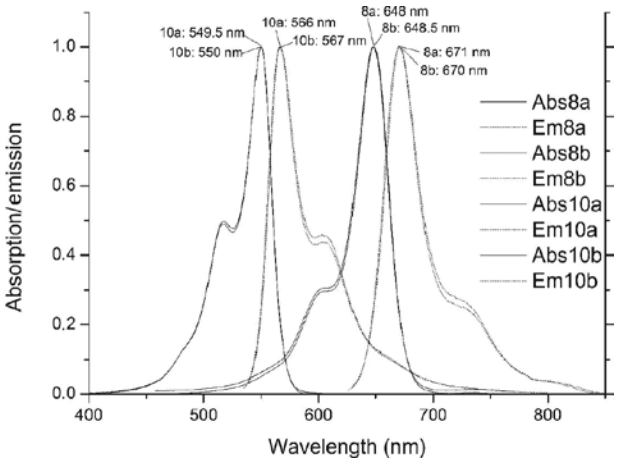

Dye compound	m	Absorption maximum (nm)	Emission maximum (nm)	Stokes-shift (nm)
8a	2	648	671	23
8b	2	648.5	670	21.5
10a	1	549.5	566	16.5
10b	1	550	567	17

4 Conclusions

A synthetic route to cyanine dyes is described. The dyes are indocyanine derivatives with a polymethine chain of five and three units, addressing absorption wavelengths at 550 and 648 nm. They are water-soluble and can be further functionalized for bioorthogonal reactions. This was demonstrated by labeling metabolically incorporated sugar-azides with the dye **8b** on the surface of living neuroblastoma cells, which were subjected to *direct* stochastic optical reconstruction microscopy (*d*STORM) for the visualization of cell-surface glycans in a nm-range. This may allow the further examination of the dynamics and spatial organization of glycans on cell-surfaces.

5 Supporting information

Chemical structures for detailed NMR characterization are given.

Acknowledgments: This work was supported by DFG SA829/13-1 (M.S.) and Se1410/6-1 (J.S.).

References

1. Ohtsubo K, Marth JD. Glycosylation in cellular mechanisms of health and disease. Cell 2006;126:855–67.
2. Haltiwanger RS, Lowe JB. Role of glycosylation in development. Annu Rev Biochem 2004;73:491–537.

3. Fuster MM, Esko JD. The sweet and sour of cancer: glycans as novel therapeutic targets. Nat Rev Cancer 2005;5:526–42.
4. Saxon E, Luchansky SJ, Hang HC, Yu C, Lee SC, Bertozzi CR. Investigating cellular metabolism of synthetic azidosugars with the Staudinger ligation. J Am Chem Soc 2002;124:14893–902.
5. Dube DH, Bertozzi CR. Metabolic oligosaccharide engineering as a tool for glycobiology. Curr Opin Chem Biol 2003;7:616–25.
6. Sletten EM, Bertozzi CR. Bioorthogonal chemistry: fishing for selectivity in a sea of functionality. Angew Chem Int Ed Engl 2009;48:6974–98.
7. Ntziachristos V. Fluorescence molecular imaging. Annu Rev Biomed Eng 2006;8:1–33.
8. Lee S, Park K, Kim K, Choi K, Kwon IC. Activatable imaging probes with amplified fluorescent signals. Chem Commun 2008:4250–60.
9. Hell SW. Far-field optical nanoscopy. Science 2007;316:1153–8.
10. Klein T, Proppert S, Sauer M. Eight years of single-molecule localization microscopy. Histochem Cell Biol 2014;141:561–75.
11. König W. Über den Begriff der "Polymethinfarbstoffe" und eine davon ableitbare allgemeine Farbstoff-Formel als Grundlage einer neuen Systematik der Farbenchemie. J Prakt Chem 1926;112:1–36.
12. Dähne S. Systematik und Begriffserweiterung der Polymethinfarbstoffe. Z Chem 1965;5:441–51.
13. Mishra A, Behera RK, Behera PK, Mishra BK, Behera GB. Cyanines during the 1990s: a review. Chem Rev 2000;100:1973–2012.
14. Mujumdar RB, Ernst LA, Mujumdar SR, Waggoner AS. Cyanine dye labeling reagents containing isothiocyanate groups. Cytometry 1989;10:11–9.
15. Wang L, Fan JL, Qiao XQ, Peng XJ, Dai B, Wang BS, et al. Novel asymmetric Cy5 dyes: Synthesis, photostabilities and high sensitivity in protein fluorescence labeling. J Photochem Photobiol A: Chem 2010;210:168–72.
16. Pham W, Medarova Z, Moore A. Synthesis and application of a water-soluble near-infrared dye for cancer detection using optical imaging. Bioconjugate Chem 2005;16:735–40.
17. Park JW, Kim Y, Lee KJ, Kim DJ. Novel cyanine dyes with vinylsulfone group for labeling biomolecules. Bioconjugate Chem 2012;23:350–62.
18. Mujumdar RB, Ernst LA, Mujumdar SR, Lewis CJ, Waggoner AS. Cyanine dye labeling reagents: sulfoindocyanine succinimidyl esters. Bioconjugate Chem 1993;4:105–11.
19. Gottlieb HE, Kotlyar V, Nudelman A. NMR chemical shifts of common laboratory solvents as trace impurities. J Org Chem 1997;62:7512–5.
20. van de Linde S, Löschberger A, Klein T, Heidbreder M, Wolter S, Heilemann M, et al. Direct stochastic optical reconstruction microscopy with standard fluorescent probes. Nat Protoc 2011;6:991–1009.
21. Heilemann M, van de Linde S, Schüttpelz M, Kasper R, Seefeldt B, Mukherjee A, et al. Subdiffraction-resolution fluorescence imaging with conventional fluorescent probes. Angew Chem Int Ed Engl 2008;47:6172–6.
22. Wolter S, Löschberger A, Holm T, Aufmkolk S, Dabauvalle MC, van de Linde S, et al. rapidSTORM: accurate, fast open-source software for localization microscopy. Nat Methods 2012;9:1040–1.
23. Bouteiller C, Clave G, Bernardin A, Chipon B, Massonneau M, Renard PY, et al. Novel water-soluble near-infrared cyanine dyes: synthesis, spectral properties, and use in the preparation of internally quenched fluorescent probes. Bioconjugate Chem 2007;18:1303–17.
24. Hilderbrand SA, Kelly KA, Weissleder R, Tung CH. Monofunctional near-infrared fluorochromes for imaging applications. Bioconjugate Chem 2005;16:1275–81.
25. Narayanan N, Patonay G. A new method for the synthesis of heptamethine cyanine dyes – synthesis of new near-infrared fluorescent labels. J Org Chem 1995;60:2391–5.
26. Flanagan JH, Jr, Khan SH, Menchen S, Soper SA, Hammer RP. Functionalized tricarbocyanine dyes as near-infrared fluorescent probes for biomolecules. Bioconjugate Chem 1997;8:751–6.
27. Mader O, Reiner K, Egelhaaf HJ, Fischer R, Brock R. Structure property analysis of pentamethine indocyanine dyes: identification of a new dye for life science applications. Bioconjugate Chem 2004;15:70–8.
28. Memmel E, Homann A, Oelschlaeger TA, Seibel J. Metabolic glycoengineering of *Staphylococcus aureus* reduces its adherence to human T24 bladder carcinoma cells. Chem Commun 2013;49:7301–3.
29. Homann A, Qamar RU, Serim S, Dersch P, Seibel J. Bioorthogonal metabolic glycoengineering of human larynx carcinoma (HEp-2) cells targeting sialic acid. Beilstein J Org Chem 2010;6:24.
30. Letschert S, Göhler A, Franke C, Bertleff-Zieschang N, Memmel E, Doose S, et al. Super-resolution imaging of plasma membrane glycans. Angew Chem Int Ed Engl 2014;53:10921–4.
31. Luchansky SJ, Hang HC, Saxon E, Grunwell JR, Yu C, Dube DH, et al. Constructing azide-labeled cell-surfaces using polysaccharide biosynthetic pathways. Methods Enzymol 2003;362:249–72.
32. Jiang H, English BP, Hazan RB, Wu P, Ovryn B. Tracking surface glycans on live cancer cells with single-molecule sensitivity. Angew Chem Int Ed Engl 2015;54:1765–9.
33. Zaro BW, Yang YY, Hang HC, Pratt MR. Chemical reporters for fluorescent detection and identification of *O*-GlcNAc-modified proteins reveal glycosylation of the ubiquitin ligase NEDD4-1. Proc Natl Acad Sci USA 2011;108:8146–51.
34. Vocadlo DJ, Hang HC, Kim EJ, Hanover JA, Bertozzi CR. A chemical approach for identifying *O*-GlcNAc-modified proteins in cells. Proc Natl Acad Sci USA 2003;100:9116–21.
35. Gurcel C, Vercoutter-Edouart AS, Fonbonne C, Mortuaire M, Salvador A, Michalski JC, et al. Identification of new O-GlcNAc modified proteins using a click-chemistry-based tagging. Anal Bioanal Chem 2008;390:2089–97.
36. Laughlin ST, Bertozzi CR. Imaging the glycome. Proc Natl Acad Sci USA 2009;106:12–7.
37. Späte AK, Bußkamp H, Niederwieser A, Schart VF, Marx A, Wittmann V. Rapid labeling of metabolically engineered cell-surface glycoconjugates with a carbamate-linked cyclopropene reporter. Bioconjugate Chem 2014;25:147–54.
38. Hein JE, Fokin VV. Copper-catalyzed azide-alkyne cycloaddition (CuAAC) and beyond: new reactivity of copper(I) acetylides. Chem Soc Rev 2010;39:1302–15.
39. Klein T, van de Linde S, Sauer M. Live-cell super-resolution imaging goes multicolor. Chembiochem 2012;13:1861–3.
40. Godin AG, Lounis B, Cognet L. Super-resolution microscopy approaches for live cell imaging. Biophys J 2014;107:1777–84.

Supplemental Material: The online version of this article (DOI: 10.1515/znc-2016-0123) offers supplementary material, available to authorized users.